Experimental and Numerical Investigation on Micro Deep Drawing Process of Stainless Steel 304 Foil Using Flexible Tools

Ihsan Irthiea*, Graham Green*, Dr Safa Hashim*, Abdulbast Kriama",

* School of Engineering, University of Glasgow, Scotland, UK,

" Mechanical and Industrial Engineering Department, College of Engineering, Al Zawiya University, Libya

Abstract

Flexible forming technology provides significant application potential in various areas of manufacturing, particularly at a miniaturized level. Simplicity, versatility of process and feasibility of prototyping makes forming techniques by using flexible tools suitable for micro sheet metal forming. This paper reports the results of FE simulation and experimental research on micro deep drawing processes of stainless steel 304 sheets utilising a flexible die. The study presents a novel technique in which an initial gap (positive or negative) is adopted between an adjustment ring and a blank holder employed in the developed forming system. The blank holder is moveable part and supported by a particular spring that provides the required holding force. The forming parameters (anisotropy of SS 304 material, initial gap, friction conditions at various contact interfaces and initial sheet thickness) related with the forming process are in details investigated. The FE models are built using the commercial code Abaqus/Standard. The numerical predictions reveal the capability of the proposed technique on producing micro metallic cups with high quality and large aspect ratio. To verify these results, number of micro deep drawing experiments is conducted using a special set up developed for this purpose. As providing a fundamental understanding is required for the commercial development of this novel forming technique, hence the optimization of the initial gap in accordance with each sheet thickness, thickness distribution and punch force/stroke relationship are detected.

Key words: Micro deep drawing, flexible die, sheet metal, FE simulation.

1. Introduction

Remarkable development in micro forming technology and relevant industries has been noticed through the last decade, mainly due to the increasing demand on high quality portable electronics and other mini/micro devices **[1-5]**. This demand has remarkably attracted a great attention from researchers **[5-7]**. Owing to provide fundamental understanding of the micro forming technology, substantial research activities have therefore been published during the last decade **[2, 8]**. Several significant potential advantages can be gained from using flexible tools in sheet metal forming processes; such as low-production cost, eliminating alignment difficulties, producing complex-shaped parts. The workpieces taken from pre-polished or painted sheet metals can be formed without using any protective coating as they. These issues make flexible forming technology very appropriate for micro sheet metal forming **[6, 9, 10]**.

To clarify the essential fundamental characteristics of this technology, several research studies have been conducted. Quadrini et al. **[11]** investigated flexible forming process of thin aluminium alloy sheets to produce simple shapes. Different rubber materials were used for the forming tools. It was found that the harder rubber pad improved the drawability of the blank material. Peng et al. **[12]** presented an experimental and numerical investigations on micro sheet metal forming of stainless steel foil using a soft punch. The effects of the process parameters of sheet grain size, rubber hardness and friction coefficients were also investigated. Dirikolu and Akdemir **[13]** established a 3D finite element (FE) model for flexible forming process of sheet metal. The rubber hardness and blank material properties were the main parameters in this work. As a result, it was shown that the FE method was effective tool in process design. Ramezani et al. **[9]** optimized theoretical approaches that can be used to simulate the static and kinetic friction at the blank and its interfaces in rubber-pad forming process. Their study showed that the use of the static friction model resulted in highly accurate predictions for the punch load while the kinetic friction model provided good results at higher forming velocities. A novel microscale laser dynamic flexible forming (μLDFF) technique is presented by Wang at el. **[14]**. Numerical simulations and experiments were carried out to investigate the key process parameters. The results showed that the deformation depth of the thin metal sheets decreases with the increase in the thickness of the soft punch. Also, it was found that increasing the laser pulse energy resulted in an increase in the deformation depth of formed workpiece.

Recently, the experience-based knowledge of the micro-forming process parameters is not sufficient, particularly when flexible tools are utilised, thus more investigations and improvements on this technology are imperatively needed **[12]**. In this paper, micro deep drawing of stainless steel (SS304) foil using a polyurethane rubber flexible forming pad, 63 Shore A hardness, is evaluated through experiments and numerical simulation. The foil work-pieces used in the experiments were each 10mm in diameter and with varying thickness as follows: 60, 100 and 150 micron. The numerical simulation was achieved using finite element analysis (FEA) model, built using the commercial code Abaqus/Standard. The main purpose of this study was to demonstrate the influence of blank material anisotropy, initial blank thickness, initial gap, and friction coefficient on the forming process. The experimental results show a good correlation with that obtained from the numerical simulations, in terms of geometrical aspects of the final products, thickness distributions and punch load-travel relationships.

2. Experimental Methodology

2.1 Characterization of material behaviour

Stainless steel 304 is used widely in various industrial applications, especially in the manufacture of micro device components. Therefore, the workpieces used in this study are intended from SS304 sheets with 60 µm, 100 µm and 150 µm in thickness. In order to evaluate the effect of the anisotropic behaviour (due to the rolling operation), dogbone-shaped specimens are cut along rolling, diagonal (45˚) and transverse directions from each thickness. The dimensions for the testing specimens are determined from the ASTM E8 standard as shown in Figure 1b.The tensile tests are performed using an Instron 5969 machine with 50kN load cell with velocity of 0.1 m/sec. A non-contacting advanced video extensometer (FOV 200mm) is utilized for measuring the longitudinal and transverse strains of the sheet specimens during the tensile test. Figure 1a presents the stress-strain relationships obtained of the tensile tests for the SS304 foils with the thicknesses 60, 100 and 150µm at rolling direction. The mechanical properties of SS 304 sheets are listed in **Error! Not a valid bookmark self-reference.**, which generally agree with the results obtained by Soatome **[5]**.

Table 1. Mechanical properties of SS304 foils

Thickness t_B(µm)	Angle to rolling direction (°)	Young modulus E (GPa)	Yield point σ_o (MPa)	Tensile strength σ_{ult} (MPa)	K (MPa)	n
60	0°	128.6	225.4	545	1252	0.4684
	45°	192.7	273.2	568	1290	0.4288
	90°	179	209.8	554.6	1299.7	0.4413
100	0°	154.5	277.2	580.5	1350.7	0.4516
	45°	197	252.3	539	1269.9	0.4340
	90°	166	287.3	621.8	1400.2	0.4103
150	0°	107.5	373	749.8	1698.2	0.4522
	45°	120.2	327.4	730.7	1585.5	0.4159

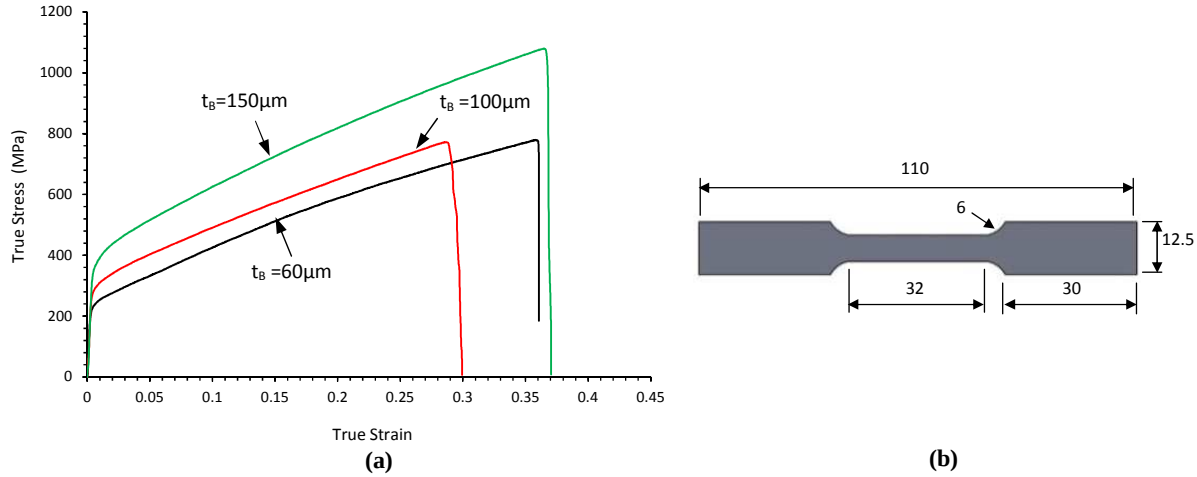

Figure 1. (a) Engineering stress-strain relationships along rolling direction (b) Tensile test sample

2.2 Compression Tests of Rubber Material

In order to define rubber material behaviour in the FE model, the mechanical properties obtained from uniaxial and volumetric compression tests are utilized. The hyperelastic coefficients of the rubber 63A material were obtained via the uniaxial compression test carried out in accordance to the ASTM D575 standard. Sandpaper sheets were placed at specimen and machine platens interfaces to resist lateral slippage of the rubber surfaces, as in Figure 2b. The engineering stress-strain relationship obtained from the uniaxial compression test can be seen in Figure 2a. Regarding the material compressibility factor (D_1), a volumetric compression test is achieved here using the device illustrated in Figure 3a. The very small clearance is to ensure that the rubber specimen used will be restricted perfectly and there is no space for the rubber to extrude through during the test **[15]**. The relationship between pressure and volume ratio that is obtained from the volumetric compression test is illustrated in Figure 3b. The results of the uniaxial and volumetric compression tests mentioned above were used as input data in the code ABAQUS/Standard to obtain the material coefficients of rubber 63A shown in **Error! Not a valid bookmark self-reference.**.

Table 2. Mechanical properties of rubber 63 Shore A hardness

Shore A	**C10 (MPa)**	**C01 (MPa)**	**D1 (MPa)**	**Poisson's ratio (v)**
63	0.586163925	0.146237297	7.79341E-04	0.499715

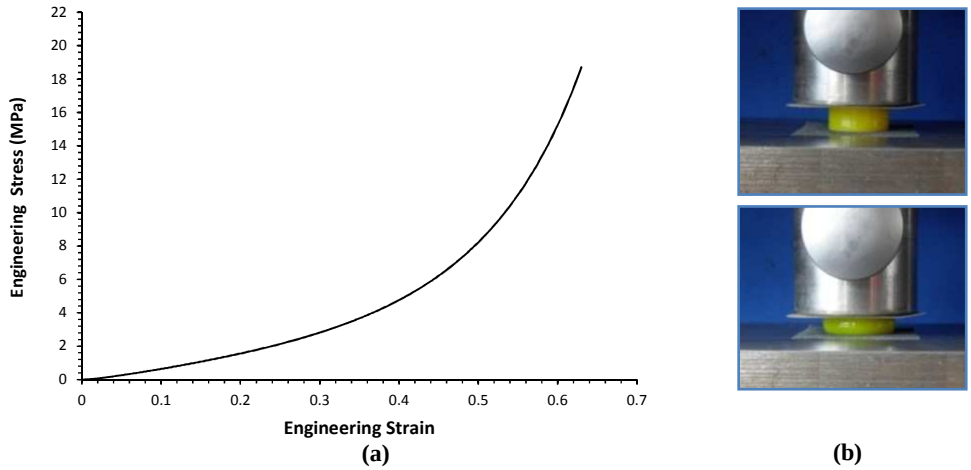

Figure 2. (a) Engineering stress strain relationship for the uniaxial compression test (b) Uniaxial compression test

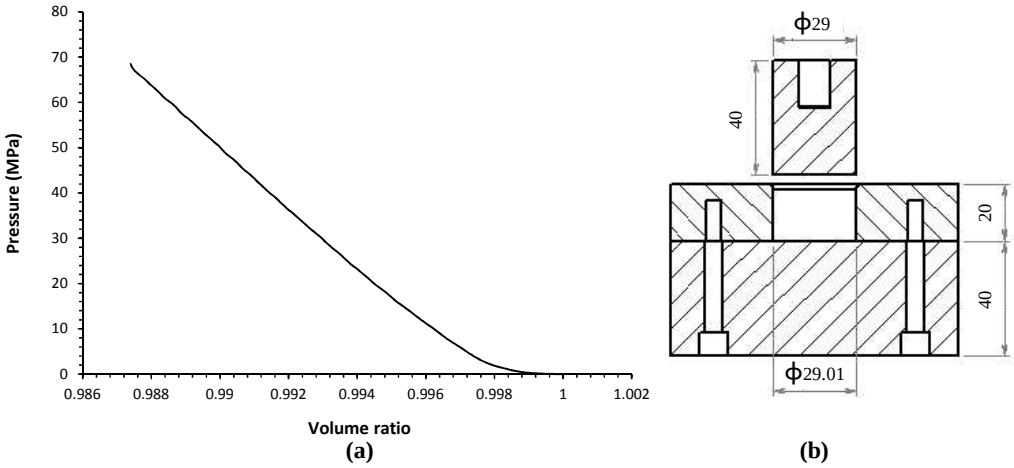

Figure 3. (a) Volume ratio-pressure relationship of rubber 63A (b) Scheme of the volumetric compression device

3. Material Models Used in FEM Simulation

3.1 Anisotropy of Stainless Steel 304 Foil

As previously mentioned, in this study FE simulations of the SS304 foil micro deep drawing process were carried out using the commercial software Abaqus/Standard. An elastic-plastic model was used to define SS304 foil behaviour in the FEA simulation. In this model, four-node doubly curved thin or thick shell, reduced integration, hourglass control elements (S4R) were used for the foil metal as illustrated in Figure 4. The plastic anisotropy is introduced by using Hill's criterion.

$$f(\sigma)=\sqrt{F(\sigma_{22}-\sigma_{33})^2+G(\sigma_{33}-\sigma_{11})^2+H(\sigma_{11}-\sigma_{22})^2+2L\sigma_{23}^2+2M\sigma_{31}^2+2N\sigma_{12}^2}$$

where F, G, H, L, M and N are material constants obtained from test tensile in different orientations and σij refers to the stress components **[16]**. These constants are defined as:

$$F=\frac{1}{2}\left(\frac{1}{R_{22}^2}+\frac{1}{R_{33}^2}-\frac{1}{R_{11}^2}\right),\quad G=\frac{1}{2}\left(\frac{1}{R_{33}^2}+\frac{1}{R_{11}^2}-\frac{1}{R_{22}^2}\right),H=\frac{1}{2}\left(\frac{1}{R_{11}^2}\right.$$

$$L=\frac{3}{2R_{23}^2},\quad N=\frac{3}{2R_{12}^2},\quad M=\frac{3}{2R_{13}^2}$$

where R_{11}, R_{22}, R_{33}, R_{12}, R_{13} and R_{23} are anisotropic yield stress ratios. In sheet metal forming, the plane stress conditions are adopted, and then just four stress ratios (R_{11}, R_{22}, R_{33} and R_{12}) are taken into account **[17]**. Within the FE code Abaqus, the anisotropic yield stress ratios are expressed in terms of width to thickness strain ratios.

$$R_{22} = \sqrt{(r_{90}(r_0+1))/(r_0(r_{90}+1))}, \quad R_{33} = \sqrt{(r_{90}(r_0+1))/(r_0(r_{90}+1))}$$

where r_0, r_{45} and r_{90} are width strain to thickness strain ratios of the work-piece material along the rolling, diagonal (θ=45˚) and transverse (θ=90˚) directions respectively. The above equations are adopted to calculate the (r) and (R) values for the SS 304 sheets employed in the current work, as shown in Error! Not a valid bookmark self-reference..

Table 3. Anisotropic plastic strain ratios

t_b (µm)	Θ (°)	r	R_{11}	R_{22}	R_{33}	R_{13}
60	0	0.975608271	1	0.97129434	0.97700096	0.94738359
	45	1.076671656				
	90	0.891692687				
100	0	0.717189264	1	0.945329304	1.02365595	0.94416213
	45	1.00371091				
	90	0.77824151				
150	0	0.759571919	1	0.98879011	1.06229062	1.01572242
	45	0.92150833				
	90	0.949827615				

3.2 Hyper-elastic Model for Rubber Pad Material

The rubber material used for the flexible die is characterised by a nonlinear stress-strain relation for large deformation, as well as it is nearly incompressible through the volumetric compression test. Therefore, the Mooney-Rivlin hyper-elastic model can be presented to describe this behaviour. Since, the total strain energy of any homogenous and isotropic material is composed from three strain invariants, the strain energy form of Mooney-Rivlin is:

$$W=C_{10}(\bar{I}_1-3) + C_{01}(\bar{I}_2-3) + (J-1)/D_1$$

where W is the strain energy per unit of volume, $\bar{I}_1$ and $\bar{I}_2$ are the strain invariants, J is volume change. C_{10} and C_{01} describe hyperelastic rubber deformation, and D_1 indicates the material compressibility **[9]**.

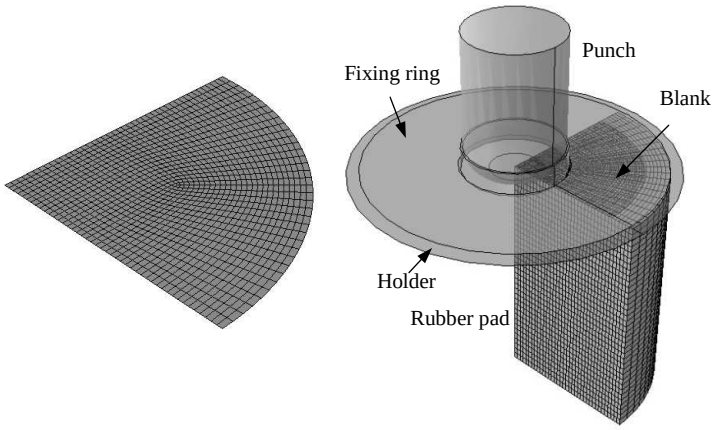

Figure 4. Simulation model of micro deep drawing process

For the rubber pad, eight-node linear brick, constant pressure, reduced integration, hourglass elements (C3D8RH) were utilized and the other parts were defined as rigid bodies as presented in Figure 4. The process geometry dimensions adopted in this study are punch diameter 4mm; punch nose radius 0.8mm, blank diameter 10mm, rubber pad diameter and height 12 and 10mm respectively. Also, the holding spring used in the current technique is modelled with 300N/mm stiffness and it is compressed to provide an initial holder force of initial 2000N. Moreover, the friction coefficients at the contact interfaces are defined in the FE simulations utilizing the coulomb friction model.

4. Experimental Setup

The special experimental set up shown in Figure 5 was developed to conduct micro deep drawing experiments. In general, this device consists of two main component sets. The first set, which represents the upper movable part of the

device, is composed of two groups of components the first group involves upper plate, three springs, three spring guiders, three guide posts, solid punch and lower plate. The second one involves the main tools responsible directly of the micro deep drawing operation, which are blank holder, blank holder house, fixing ring and holding spring. This set is driven by the movable grip of the Instron 3956 machine, where the load and displacement can be acquired directly from the Bluehill software provided with this machine.

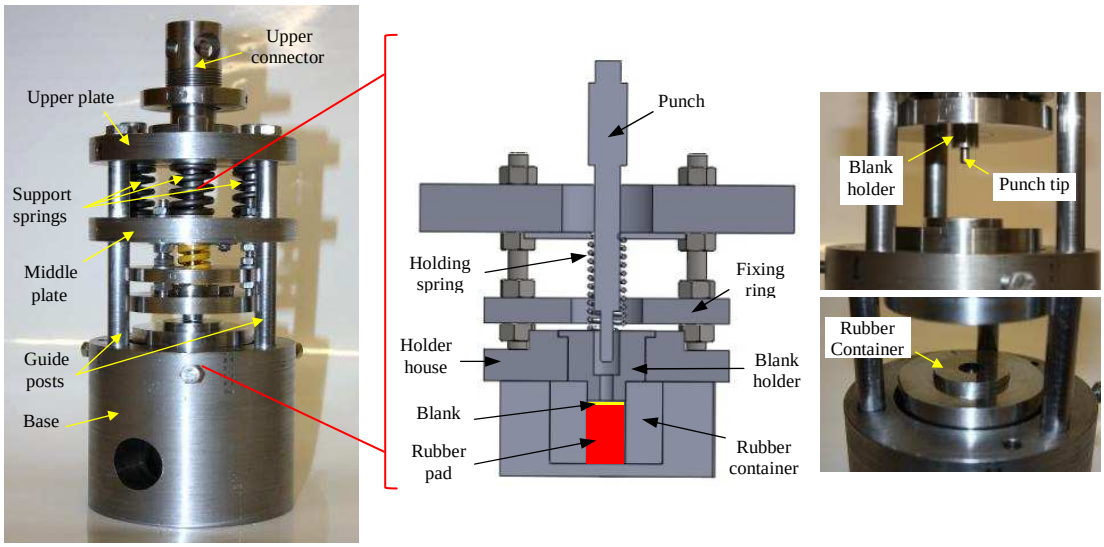

Figure 5. The experimental apparatus

The second set is constructed of a solid base, rubber container and rubber pad. The main function of the three springs is to keep the flange portion of the blank holder in direct contact with rubber container surface during the drawing stroke. Therefore, these springs have a relatively high stiffness of 300 N/mm, which is enough to overcome any possible movement of the middle plate upward. The Surtronic 3P Taylor-Hobson roughness tester is used to measure the surface roughness of the components employed in the experiments. The forming rigid tools are equipped with surface roughness degrees of 1.41µm and 2.97µm forthe blank holders and the punch respectively, whereas the SS 304 sheets were finished with approximately 0.64µm.

5. Experimental Procedure

The blanks used in the micro deep drawing processes were cut from the SS 304 foils using a blanking punch-die tool. In order to obtain good cutting quality a clearance about 12-24% of the initial sheet thickness was adopted between the male-female blanking tools **[18]**. Before the actual forming stroke; the three springs are initially compressed provide sufficient supporting force for the middle plate. Thereafter, this force increases simultaneously with the drawing stroke. The forming procedure, shown in Figure 6a, is carried out with a positive initial gap and can be summarized in the following steps: *Step* 1: The rigid punch is moved downward just to contact the blank surface. *Step* 2: In this step the punch deform both the blank and rubber pad just through the initial gap adopted. As a result of incompressibility of the rubber material, a hydrostatic pressure will be generated in the rubber pad keeping the formed part of the blank in continuous contact with the rigid punch. Since the rubber pad is restrained inside a closed cylindrical space the resulting pressure pushes both the blank flange and blank holder upwards through the gap against the holding spring. Through this step the contact area between the blank flange and the holder decreases causing the holding force to decrease. As a result, the compromise between the decreasing contact area and the increasing rubber pressure is a very important aspect in this technique. *Step* 3: The final step of the drawing operation starts just when the blank holder reaches the fixing plate. At this moment the rubber container is completely closed a high forming load is needed to resist the high reaction pressure of the rubber pad. Afterwards, the rigid punch is kept moving down to finish drawing stroke.

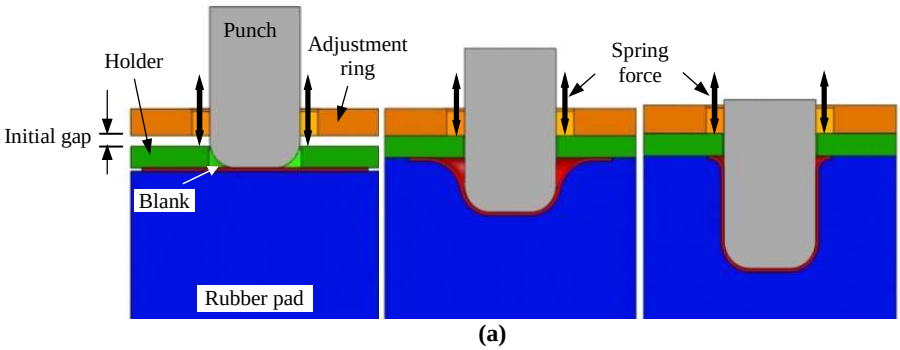

(a)

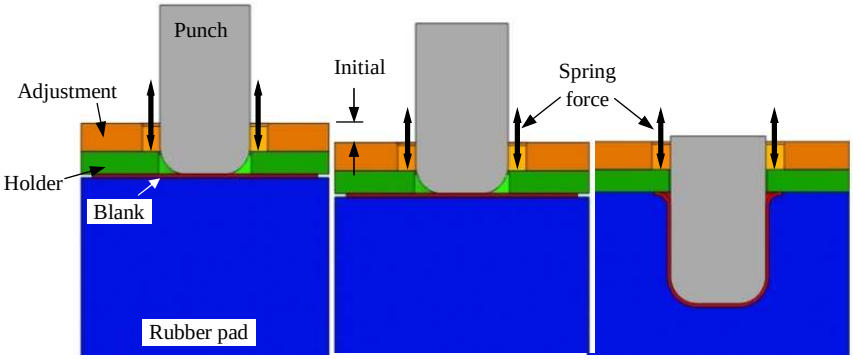

Figure 6. Forming techniques with (a) positive initial gap and (b) negative initial gap

In some cases where an initial compression is required to be established the experimental procedure illustrated in Figure **6**b is utilized. *Step* 1: The rigid punch is moved downward just to contact the blank surface. *Step* 2: All of the rigid punch, blank holder and fixing plate are moved downward for the required initial compression distance (negative gap). This technique generates an initial pressure (pre-bulging pressure) in the rubber pad. *Step* 3: In this step both the blank and the rubber are formed by the rigid punch, producing a complete cup. An important note here is that the incremental increase in the forming load in this technique is higher than that obtained in the step 3 of the previous one because the rubber pad here is initially compressed.

6. Results and Discussion

Figure 7 shows cups obtained from FE simulations and experiments with blanks of 100 µm in thickness and final depth 4 mm for no initial gap adopted. The physical cups expose well correlation with that acquired from the numerical models in terms of final geometrical profile. During the drawing process, the blank being formed is held at the flange region and the bottom as seen in Figure 6a, and consequently the cup shoulder and the upper portion of the side wall would undergo excessive tension conditions. Therefore, it can be observed from Figure 7b that the maximum tensile stresses are concentrated at these critical regions of the formed cup, while the flange region experiences high frictional shear stresses.

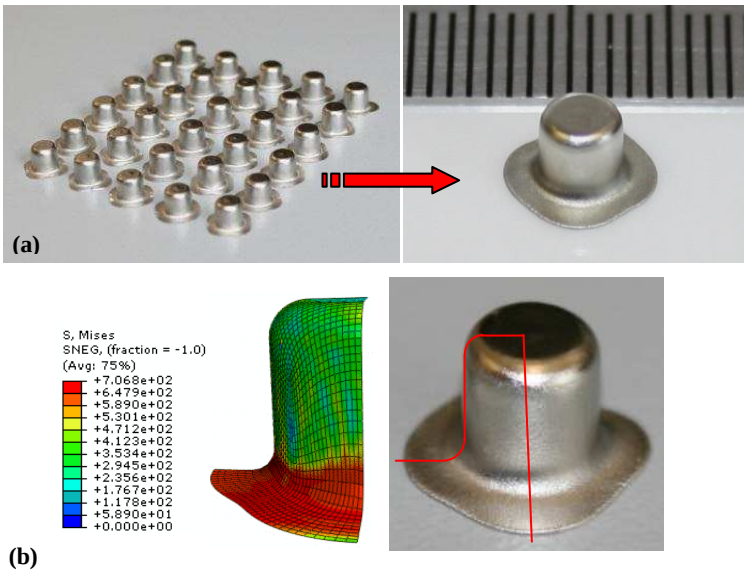

Figure 7. Drawn cups obtained from (a) experiment (b) simulation

Moreover, the effect of the anisotropic behaviour of the SS304 sheet material of 100 µm in thickness is shown in Figure 8. In this figure, the thickness distributions of drawn cup along the rolling, diagonal 45˚ and transverse directions are presented. The first finding is that the bottom wall almost remains without change in thickness. The forming pressure is initially applied on the blank portion underneath the punch nose, and since the friction coefficient punch surface is relatively high, hence the frictional forces excited at this region will overcome any possible relative

sliding. This action implies no increasing tensile forces would generate at the bottom at which therefore no significant thinning occurs. The current technique allows for the blank to form as a shallow cup in the next step, and therefore the cup undergoes nearly the same reduction in thickness along the three different directions. Thereafter, since the cup becomes in direct contact with the punch nose radius, the same scenario mentioned above for the bottom region can be adopted thus the wall thickness remains without noticeable change at this region.

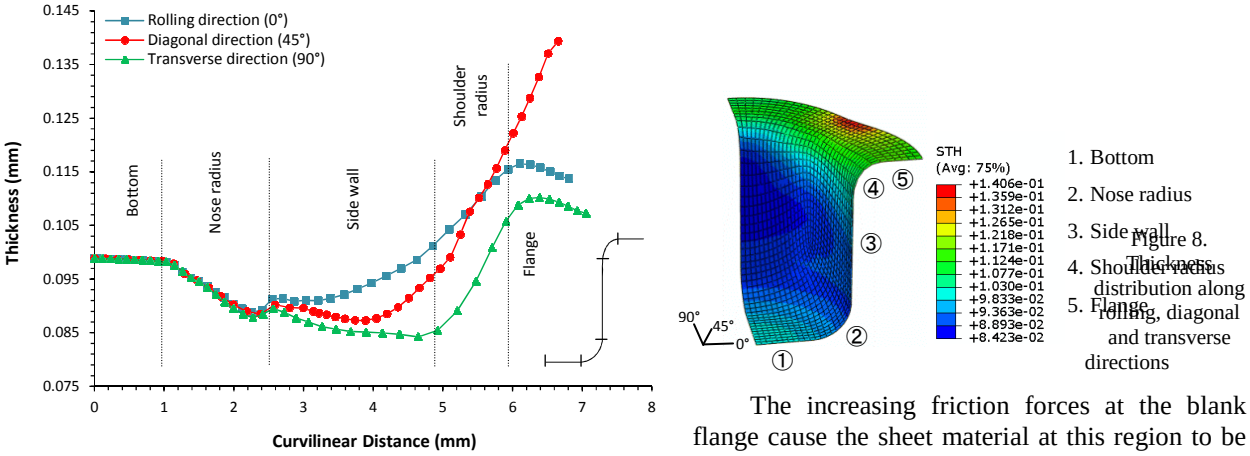

Figure 8. Thickness distribution along rolling, diagonal and transverse directions

The increasing friction forces at the blank flange cause the sheet material at this region to be radially swept away towards the outer periphery. This activity results in the cup wall goes up to higher thickness relatively at shoulder radius and significantly in flange region. The curves show that the maximum thinning is observed at the transverse direction (90° to the rolling direction) at the upper part of the cup side wall, which is contrary to the conventional deep drawing process where the maximum thickness reduction is usually observed at the punch nose radius. In order to compare the numerical results with that obtained from the experiments, Figure 9a shows a physical cup cut at rolling and transverse directions. Figure 9b presents a comparison between the simulation predictions and experimental results in terms of thickness distribution along directions aforementioned. It can be noted that the tendency of change in thickness predicted by numerical model match well with that given by experiments, where both results detect that the maximum thinning is at the cup side wall along the transverse direction. Thus, the thickness distribution along just this direction will be taken into account in the next sections. However, little differences in thickness between the numerical and experimental results can be observed, which could be due to the difficulty in manufacturing the physical tools with surface roughness result in friction coefficients equalling exactly to that adopted in the numerical models which are 0.1 and 0.25 at the blank-holder and blank-punch interfaces, respectively.

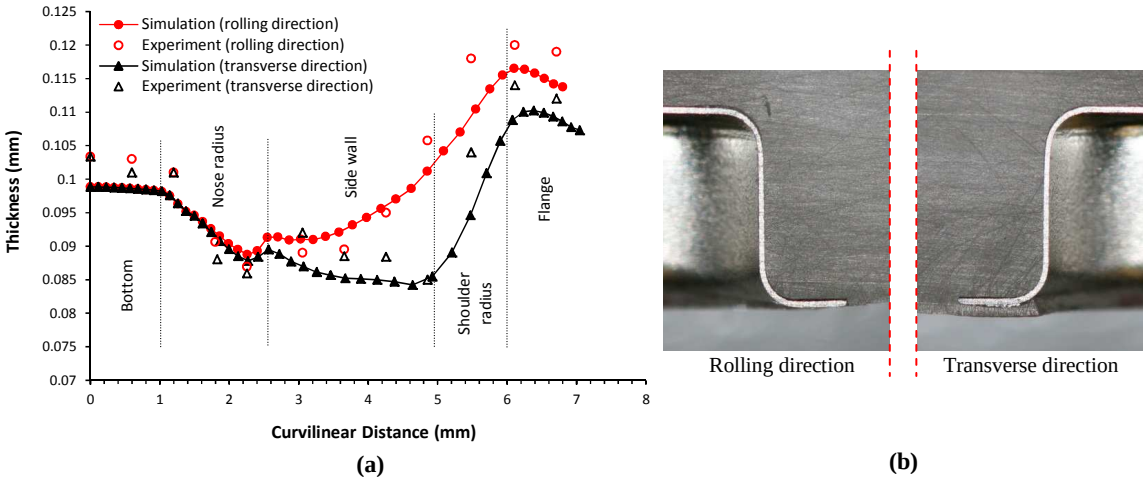

Figure 9. (a) Thickness distribution along rolling and transverse directions (b) Two sections of a physical cup

6.1 Initial Gap

Of the most crucial parameters in the proposed micro deep drawing technique is the initial gap allocated between the blank holder and the adjustment ring. In order to study the influence of this parameter, different initial gaps of -100, -50,0, 50 and 100 µm) are adopted under the same process conditions. The numerical simulation results reveal some variations in the geometrical profiles of the obtained cups, where increasing the initial gap results in a larger radius for the shoulder corner of the formed cups. Another observation is that the heights of the final cups are slightly different where the cup height increases by the same value of the initial gap adopted. The thickness distributions along the

transverse direction, which predicted by the simulations with the different gaps aforementioned are presented in Figure 10. It can be seen that reducing the initial gaps causes an increase in thickness reduction especially at the side wall of the formed cup. The results detect that the maximum reduction in the side wall thickness decreases from 15.8% to 11.9% by increasing the initial gap from 0 to 100 µm, as well as increases from 15.8% to 28% by reducing the gap from 0 to -100 µm. The interesting attention is that the location of the maximum thinning changes from the nose radius to the upper part of the side wall of the final cups with reducing the initial gaps. This action can be attributed that reducing the initial gap exacerbates restriction on the rubber pad material. As a result of rubber compressibility, smaller gap causes the pressure applied by the rubber die, which is in fact regarded blank holding pressure in the current technique, on the blank to significantly increase. Thereby, higher tensile stresses therefore generate at the side wall and shoulder radius of the cup being formed during the drawing operation, resulting in an increase in thickness reduction which leads to failure by fracture. Therefore, it can say that formability of the workpiece can be improved by adopting higher initial gaps. However, it should be realized that the gap values are limited; i.e. it cannot be increased as much as we want, where the results reveal that adopting gap of ≥110 µm for the current case produces wrinkled parts.

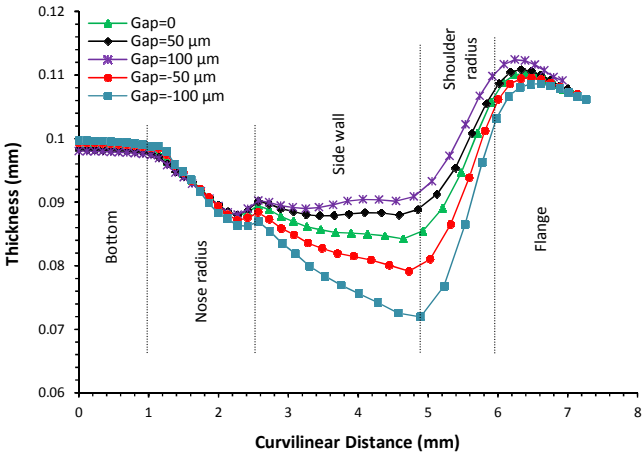

Figure 10. Thickness distribution at transverse direction for different gaps

On the other side, the punch load-travels results report that the punch load increases throughout the drawing stroke until reach the maximum value when a completed cup is obtained. Another observation is that the punch load value at any particular forming stage decreases with increasing the initial gap as shown in Figure 13. The results showed that the maximum load decreases from 3682 N with the negative gap -100 µm to 2320.7 N with no initial gap, and then to 2007.5 N with the initial gap 100 µm. On explanation of these results, it can be said that as the initial gap increases, blank and the rubber pad will have larger space to deform against just the supporting spring. This situation allows drawing as much as possible of the blank material into the rubber die cavity before the holder reaches the stationary adjustment ring. Since the area of the flange region reduces increasingly during the drawing stroke, the friction forces at the blank/holder and blank/rubber pad interfaces will therefore decrease leading to reduction in the maximum tensile stresses generated in the blank material. Consequently, the thinning and the maximum punch load will decrease. Figure 11 presents three physical cups produced with the initial gaps -100, 0 and 100 µm. It can be seen how the different initial gaps affect the final cup profiles in particular at the shoulder corner radius.

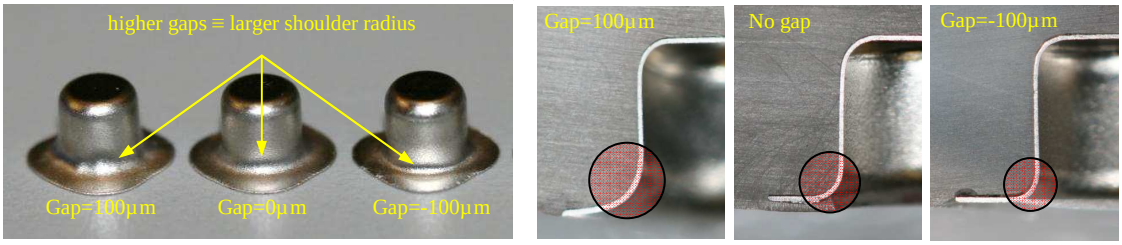

Figure 11. Cups formed with different initial gaps

Figure 12 reveals a comparison between thickness distributions along the transverse direction obtained from FE simulations and experiments for cups formed with these gaps. Although there are little variations in thickness values at some locations, however the general trend of the change in predicted thickness distribution well matches with the experimental results.

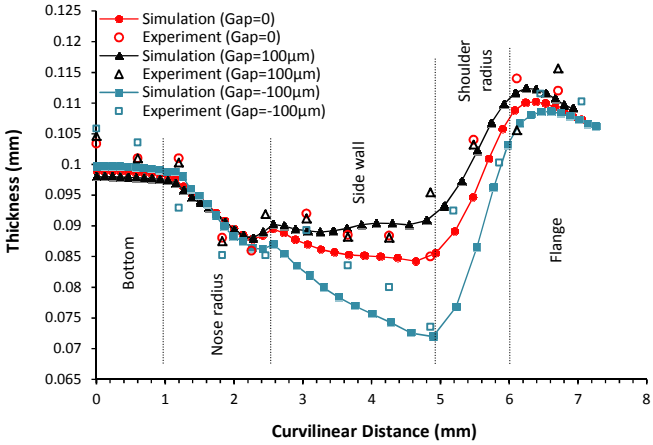

Figure 12. Thickness distributions along transverse direction with different initial gaps

Regarding the drawing load, Figure 13 illustrates comparisons between the punch load-travel relationships obtained from simulation and experimental work for the different gaps aforementioned. It is found that the maximum punch loads required for experiments are higher than those in the simulations. The differences between the drawing load-stroke curves could be due to the difficulty of setting friction coefficients for the experiments exactly equal to that adopted in the numerical models. In addition, the developed set up consists of various parts that are in direct contact with each other and hence the friction between them, which is not taken into account in the FE models, possibly leads to increasing in total load measured by the experiment machine used. The results detect that the punch loads measured through experiments are 9.5%, 10% and 8.1% higher than numerical results with the initial gaps 100, 0 and -100 µm, respectively.

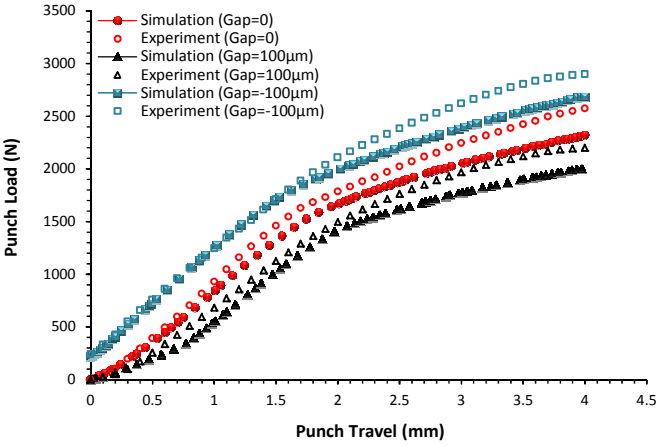

Figure 13. Comparison of Punch load-travel relationships with different initial gaps

The initial gap therefore significantly influences on the production quality of the final cups in terms of thickness distributions and thing values, as well as on the maximum forming load. In accordance with these results, it is found that owing to produce cups of similar profiles with 0.75, 1 and 1.25 aspect ratio (i.e. final depths of 3, 4 and 5mm), the initial gaps of -100 µm, -50 µm and 0 respectively can be adopted as shown in Figure 14. In fact, the maximum aspect ratio which can be achieved for the blank diameter of 10mm used in the current investigation is 1.25, where no enough material remaining at the flange region to produce a free-earing cup. It is reported in a previous work **[19]** that it cannot produce SS 304 cups at micro scale with high aspect ratio; that is >1, through a conventional deep drawing process by using a single forming die. Thus, the aspect ratio of 1.25 achieved by adopting the proposed technique through a single deep drawing process using a rubber die indicates that this technique is noticeably more efficient than the conventional deep drawing in terms of manufacture cost and production time.

Figure 15 reveals the thickness distributions along the transverse direction for the two groups of the cups illustrated in Figure 14, which are obtained from FE models and experiments. It can be seen that the maximum thinning occurs at the side wall along the transverse direction even for the cup drawn to 3mm depth. Unlike to the conventional micro deep drawing processes, the results indicate that the lowest maximum thinning is observed for the cup of 5mm final depth whereas the highest thinning occurs for the cup of 3mm depth. This strange action is in fact due to the initial gaps adopted with each case, where the where the smallest gap results in the highest thinning and the largest gap results in lowest thinning regardless the final depth targeted for the cups formed in the current investigation. This observation refers to the significant role of the initial gap on the formability of the sheet metal and on the quality of the produced parts. It can be deduced that the initial gap is more effective than the drawing stroke. The results show that the

variations in the maximum thinning between the simulation and experimental results are 2.6%, 1.89% and 2.1% with the aspect ratios 0.75, 1 and 1.25, respectively.

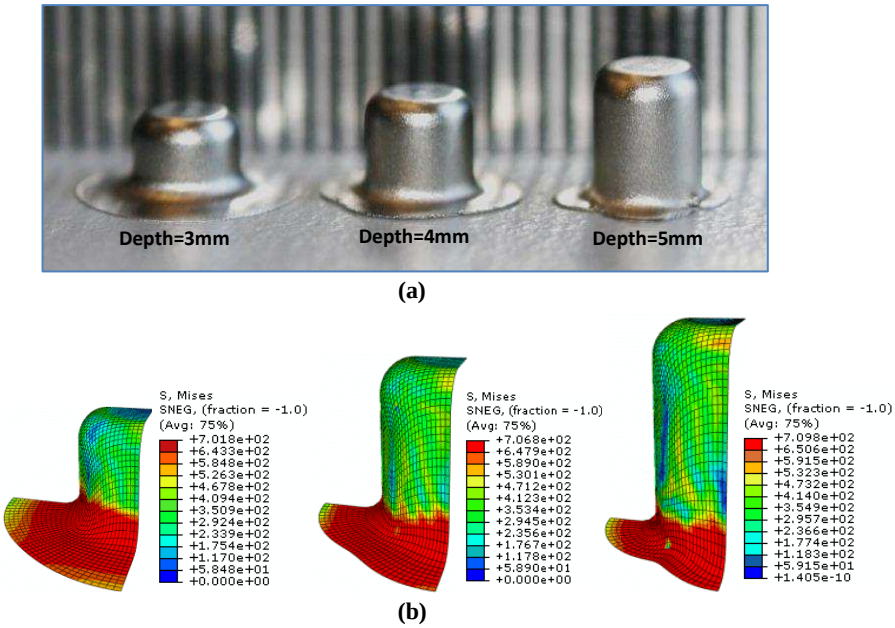

Figure 14. (a) Physical cups and (b) VonMises stress distributions for cup models with different final depths

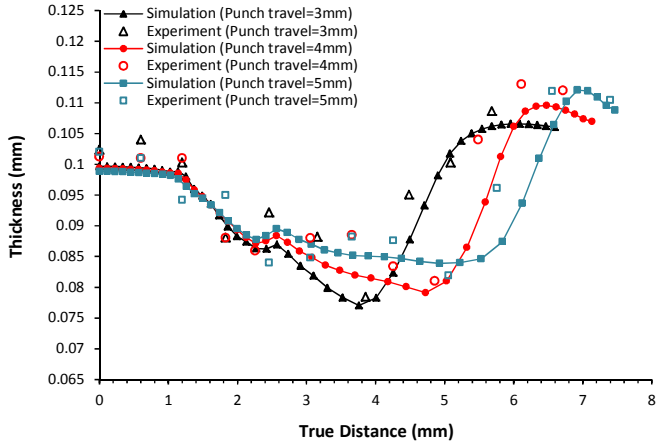

Figure 15. Thickness distributions along the transverse direction with different drawing strokes

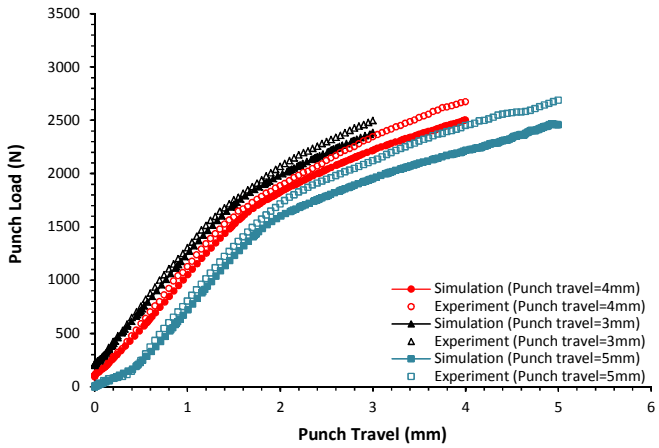

Figure 16. Comparison of punch load-travels relationships for different drawing strokes

The punch load-travel relationships presented in Figure 16 demonstrates that higher increments in the punch load values throughout the entire drawing stroke are obviously observed for the curve of punch travel 3mm, in return

the lowest increments are for the curve of punch travel 5mm. However, the highest value of the maximum punch load is reported for the case of 5mm cup depth whereas the smallest one is for the case of 3mm stroke. This finding indicates that the incremental increase in the punch load is mainly affected by initial gap value and however the maximum load is affected by the forming stroke targeted in a particular case. The last action is attributed that a higher drawing stroke results in a higher hydrostatic pressure in the rubber die material which necessitates higher punch load to keep forming both the blank and the rubber material. The result indicates that the numerical predictions for all cases of punch strokes match well with the experimental results, although the experimental curves are slightly higher than the numerical ones.

6.2 Friction Coefficient

One of the most crucial parameters in micro deep drawing processes is the friction coefficient between blank and forming tools. The friction conditions at the contact interfaces in sheet metal forming processes have a significant influence on the sheet formability and production quality of the formed parts. Due to the so called "size effects" friction coefficients play more effective role on forming results at micro scale much more than conventional scaled **[20-22]**. In the current work, the influence of friction conditions are studied through numerical simulations by using the Coulomb friction model with different values separately for each friction coefficient at the blank/holder, blank/rubber and blank/punch contact interfaces. In regard of the effect of the friction coefficient (μ_{BH}) at the blank/holder interface, the values 0 and 0.25 are defined for the friction coefficients at the blank/rubber and blank/punch interfaces respectively. Figure 17a shows the thickness distribution along the transverse direction of the formed cups acquired with different μ_{BH} values. As seen the curves have almost the same basic features. Also, no remarkable change can be observed in the thickness of the cup bottom portion for all cases, and however the differences in thinning become more distinct starting at the cup nose corner. It can be noticed that the maximum thinning of the products increases with increasing the friction coefficient μ_{BH}. The maximum reduction in thickness of the cup formed with μ_{BH}=0 is 10% at the cup nose corner region in return of 33% with μ_{BH}=0.2 at the cup side wall. The mechanism behind this behaviour is that as the friction coefficient increases, the obstructions of the frictional forces to the relative motion between the blank and its holder increases, resulting in excessive tensile stresses in the sheet material. These maximum tensile stresses resulted of μ_{BH}=0.25 exceed the ultimate tensile stress of the used SS 304 sheet metal, which cause the formed cup to break at drawing stroke of 2.6 mm. In addition, the results detect that the μ_{BH} slightly influence on the maximum punch load required where the maximum load 2088 N at μ_{BH}=0 increased to 2236 N at μ_{BH}=0.2 which means just 6.6% increase.

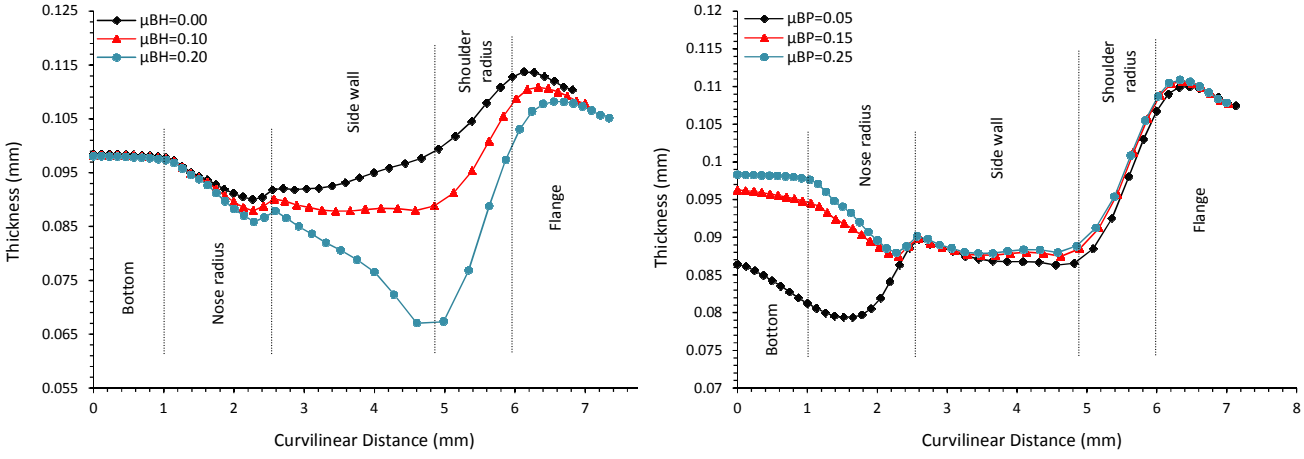

Figure 17. Thickness distribution along transverse direction with different values for the friction coefficients (a) μ_{BH} and (b) μ_{BP}

On the other side, It is found that varying the friction coefficient at the blank/rubber die has no noticeable effect on the maximum reduction in thickness of the final parts and also on the maximum punch load. The reason of these findings is that the rubber material deforms instantaneously along with the sheet metal during the drawing operation, this activity causes the relative motion at the blank/rubber interface to be very small which implies no high friction forces would be excited there. Thus, it can be deduced that the influence of the friction conditions at the blank/rubber die interface on the micro drawing process can be neglected. In order to reveal the effect of the friction coefficient (μ_{BP}) at blank/punch interface, the friction coefficients μ_{BH} and μ_{BR} are defined with 0.1 and 0 respectively. Figure 17b shows that the very affected regions by this parameter are the bottom and the nose corner of the formed cup. The strange finding in this figure is that higher maximum reduction in thickness is obtained with lower friction coefficient (μ_{BP}=0.05). Nevertheless, the results reveal that the cup formed with μ_{BP}=0 is broken at nearly its nose corner portion. The reason of this behaviour is that as the friction coefficient μ_{BP} decreases the relative motion between the blank and the punch increases, causing the blank being formed to experience excessive tensile stresses which result in fracture with μ_{BP}=0. It is detected that the maximum reductions in thickness 13.6%, 3.7% and 1.7% at the cup bottom

and 20.6%, 8.9%, and 6.8% at the most affected part of the nose corner are observed with μ_{BP}=0.05, 0.15and 0.25 respectively.

6.3 Blank Thickness

Stainless steel 304 sheets with different thicknesses of 60 µm, 100 µm and 150 µm are in this study, which implies that the punch diameter to blank thickness ratios are 66.67, 40 and 26.7, respectively. In fact, this ratio significantly influence on the drawability of this metal sheets **[20]**. At the beginning, Owing to investigate the effect of the initial sheet thickness on the drawing process, μ_{BH}=0.1 and μ_{BR}=0 with initial gap of 50 µm are adopted. The results reveals that the cup formed from the sheet of 100 µm in thickness is successful and however the one with 150 µm in thickness is just shallow at the shoulder radius, while no successful cup can be produced with 60µm sheet thickness under the given conditions due to fracture, as shown in Figure 18. In order to obtain a reasonable comparison between cups formed from the aforementioned sheets, the final profiles of the cups should be the same and the process conditions therefore are changed so that μ_{BH}=0.05 and μ_{BR}=0, and the initial gaps of 60, -100 and -550 µm are adopted for the sheet thicknesses 60 µm, 100 µm and 150 µm, respectively.

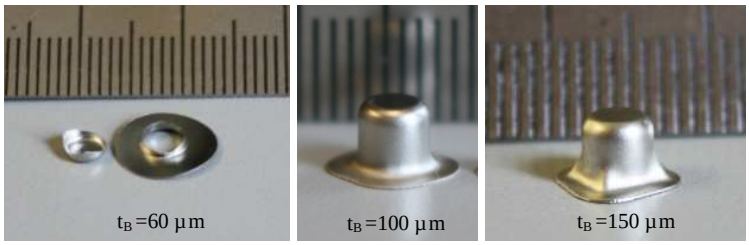

Figure 18. Stress distribution predicted by simulation with blank thickness (t_B)

Figure 19 demonstrates the thickness distributions along the transverse direction, obtained from FE simulations and experiments for cups formed with different initial thicknesses. The curves show that the bottom regions remain without remarkable change in thickness while the maximum thinning is found at the cup side wall for the three different thickness cases. It can be observed that the cup formed from the sheet of 60 µm in thickness has the best uniform wall thickness along the adopted path exception the flange portion that experience noticeable thickening, whereas clear thinning is detected at the side wall and also at the nose corner of the cups with 100 µm and 150 µm in thickness.

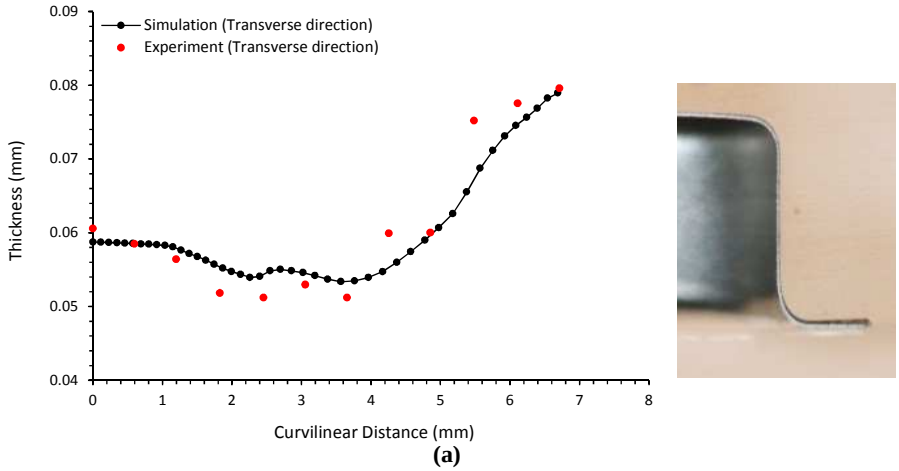

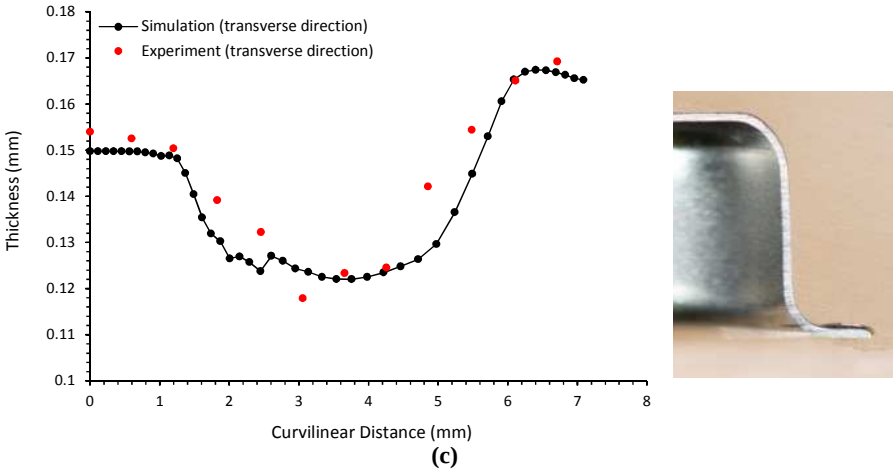

Figure 19. Thickness distributions along the transverse direction with initial blank thickness of (a) 60µm (b) 100µm and (c) 150µm

The maximum thinning occurred for the cup with initial sheet thickness of 150 µm is the highest although it is the thickest one used in this study, which could be due to the high negative gap -550 µm adopted for this case. An important finding is that the variation between the thinning values observed for the cup wall with 150 µm initial thickness of is very slight compared with the other cases, which indicates that the anisotropy nature of sheet materials is affected by the initial thickness of the utilized sheet. The maximum reductions in thickness obtained from the numerical simulations are 11%, 11.48% and 16.4% in return of 14.6%, 15% and 17.9% obtained from experiments for initial blank thickness of 60, 100 and 150 µm respectively. Regarding the maximum punch load required to produce successful cups, the results indicate that the maximum load value increases significantly with the increase in initial blank thickness as seen in Figure 20. The numerical results reveal that the maximum punch loads required to produce cups with 60, 100 and 150 µm blank thickness are 1929.5, 2878 and 5158.8 N respectively.

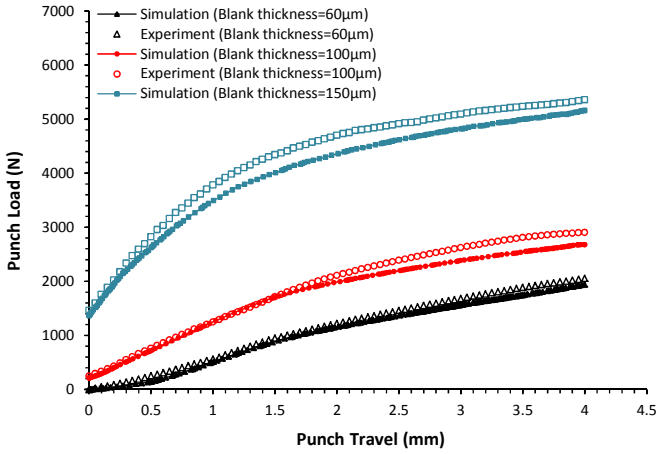

Figure 20. Comparison of punch load-travel relationship obtained for different initial blank thicknesses

The important finding in this figure is that the curves referring to the initial thicknesses 100 and 150 µm start with particular load values 332 N and 1367 N, respectively. In addition to the influence of the initial blank thickness itself, the reason of this action is the negative initial gaps adopted for these cases, which cause the rubber die material to be compressed with an initial hydrostatic pressure that require an initial punch load to overcome. Moreover, Figure 20 indicates that the punch load curves obtained from the experiments are slightly higher than the simulation predictions. The results show that the maximum loads given by experiments are 2056.1 N, 3024.6 N and 5356.8 N for the cases of the different initial blank thicknesses 60, 100 and 150 µm, respectively.

7. Conclusion

This paper presents an experimental and FE numerical study on forming micro stainless steel 304 cups by utilizing the technology of flexible tools. A novel technique is proposed in this work through adopting an initial gap (positive or negative) between the adjustment ring and the blank holder involved in the developed deep drawing system. The hydrostatic pressure, which is excited in the flexible die material due to the punch action, causes the blank holder to move up against the spring force. It was observed that the anisotropic behaviour of the SS 304 sheets has an important role on the quality of the formed parts in terms of wall thickness distribution along different paths with respect to the

rolling direction. It was found that the maximum thinning occurs at cup side wall along the transverse direction. Also, the results showed that reducing the initial gap causes an increase in the maximum thinning of the final products. Therefore, it is recommended for the thin sheets to adopt relatively big initial gaps but not more than a particular limit as may leads to excessive wrinkles at the shoulder corner and the flange region. Larger friction coefficient between the blank and the holder results in higher cup thinning at the side wall and the shoulder corner that decreases the formability, whereas the friction coefficient between the blank and the flexible die dose not play an important role. In addition, smaller friction coefficient between the blank and the rigid punch make the obtained cup thinner at the bottom and the nose corner. Thus, it is strongly recommended to fabricate the rigid punch with rough surface and the blank holder with smooth surface. As proven by this study, stainless steel 304 cups with large aspect ratio can be obtained by the proposed process, through a single micro deep drawing stage using flexible die. This action cannot be achieved by the conventional deep drawing technology unless multi stage micro deep drawing is adopted which necessitates different forming punch and die sets. As a result, this proposed technique will make the production of micro metallic cups of significantly lower overall cost and high quality.

8. References

[1] **Fung-Huei Yeh, Ching-Lun Li and Yuung-Hwa Lu,** "*Study of thickness and grain size effects on material behavior in micro-forming*", Journal of Materials Processing Technology, vol. 201, pp. 237-241, **2008**.

[2] **Frank Vollertsen, Zhenyu Hu, Hendrik Niehoff, H. Schulze and Carmen Theiler,** "*State of the art in micro forming and investigations into micro deep drawing*", Journal of Materials Processing Technology, vol. 151, pp. 70-79, **2004**.

[3] **L. V. Raulea, A. M. Goijaerts, L. E. Govaert and F. P. T. Baaijens,** "*Size effects in the processing of thin metal sheets*", Journal of Materials Processing Technology, vol. 115, pp. 44-48, **2001**.

[4] **Linfa Peng, Fang Liu, Jun Ni and Xinmin Lai,** "*Size effects in thin sheet metal forming and its elastic–plastic constitutive model*", Materials & Design, vol. 28, pp. 1731-1736, **2007**.

[5] **Yasunori Saotome, Kaname Yasuda and Hiroshi Kaga,** "*Microdeep drawability of very thin sheet steels*", Journal of Materials Processing Technology, vol. 113, pp. 641-647, **2001**.

[6] **Yanxiong Liu, Lin Hua, Jian Lan and Xi Wei,** "*Studies of the deformation styles of the rubber-pad forming process used for manufacturing metallic bipolar plates*", Journal of Power Sources, vol. 195, pp. 8177-8184, **2010**.

[7] **Chi-Han Chen, Jenn-Terng Gau and Rong-Shean Lee,** "*An Experimental and Analytical Study on the Limit Drawing Ratio of Stainless Steel 304 Foils for Microsheet Forming*", Materials and Manufacturing Processes, vol. 24, pp. 1256-1265, 2009/12/21 **2009**.

[8] **U. Engel, E. Egerer and M. Geiger,** "*Production of Microparts by Cold and Warm Forming*", in Proc. of the CIRP Seminar on Micro and Nano Technology, pp. 69-72, **2003**.

[9] **Maziar Ramezani, Zaidi Mohd Ripin and Roslan Ahmad,** "*Computer aided modelling of friction in rubber-pad forming process*", Journal of Materials Processing Technology, vol. 209, pp. 4925-4934, **2009**.

[10] **S. Thiruvarudchelvan,** "*Elastomers in metal forming: A review*", Journal of Materials Processing Technology, vol. 39, pp. 55-82, **1993**.

[11] **Fabrizio Quadrini, Loredana Santo and Erica Anna,** "*Flexible forming of thin aluminum alloy sheets*", International Journal of Modern Manufacturing Technologies, vol. II, pp. 79-84, **2010**.

[12] **Linfa Peng, Peng Hu, Xinmin Lai, Deqing Mei and Jun Ni,** "*Investigation of micro/meso sheet soft punch stamping process – simulation and experiments*", Materials & Design, vol. 30, pp. 783-790, **2009**.

[13] **M. Husnu Dirikolu and Esra Akdemir,** "*Computer aided modelling of flexible forming process*", Journal of Materials Processing Technology, vol. 148, pp. 376-381, **2004**.

[14] **Xiao Wang, Daozhong Du, Hu Zhang, Zongbao Shen, Huixia Liu, Jianzhong Zhou, Hui Liu, Yang Hu and Chunxing Gu,** "*Investigation of microscale laser dynamic flexible forming process—simulation and experiments*", International Journal of Machine Tools and Manufacture, vol. 67, pp. 8-17, **2013**.

[15] **Gregory L. Bradley, Peter C. Chang and Andrew W. Taylor,** "*Determination of ultimate capacity of elastomeric bearings under axial loading*", Report to United State Department of Commerce, National Institute of Standardsand Technology (NIST) **1998**.

[16] **A. Le Port, F. Toussaint and R. Arrieux,** "*Finite element study and sensitive analysis of the deep drawing formability of commerciallypure titanium*", International Journal of Material Forming, vol. 2, pp. 121-129, **2009**.

[17] **D. V. Hai, S. Itoh, T. Sakai, S. Kamado and Y. Kojima,** "*Experimentally and Numerical Study on Deep Drawing Process for Magnesium Alloy Sheet at Elevated Temperatures* ", Materials Transactions, vol. 49, pp. 1101-1106, **2008**.

[18] **Unipunch Speed Within Reach,** (**2012**), "*http://www.unipunch.com/PartsBook/TechnicalInformation.aspx*".

[19] **Jenn-Terng Gau, Sujith Teegala, Kun-Min Huang, Tun-Jen Hsiao and Bor-Tsuen Lin**, "*Using micro deep drawing with ironing stages to form stainless steel 304 micro cups*", http://www.sciencedirect.com/science/article/pii/S1526612513000236, **2013**

[20] **F. Vollertsen, H. Schulze Niehoff and Z. Hu,** "*State of the art in micro forming*", International Journal of Machine Tools and Manufacture, vol. 46, pp. 1172-1179, **2006**.

[21] **Linfa Peng, Dong'an Liu, Peng Hu, Xinmin Lai and Jun Ni,** "*Fabrication of Metallic Bipolar Plates for Proton Exchange Membrane Fuel Cell by Flexible Forming Process-Numerical Simulations and Experiments*", Journal of Fuel Cell Science and Technology vol. 7, pp. 0310091-9, **2010**.

[22] **Ulf Engel,** "*Tribology in microforming*", Wear, vol. 260, pp. 265-273, **2006**.